Fuel Cell System Control under Converter Losses with Experimental Results

M. Ghanes * **O. Bethoux** ** **M. Hilairet** *** **J-P. Barbot** *

* *Laboratoire d'Electronique et Commande des Systèmes ECS -Lab EA 3649, ENSEA 6, Avenue du Ponceau 95014, Cergy-Pontoise cedex*
** *Laboratoire de Génie Electrique de Paris (LGEP) / SPEE-Labs, CNRS UMR 8507; SUPELEC; Université Pierre et Marie Curie P6; Université Paris-Sud 11; 11, rue Joliot Curie, Plateau de Moulon F91192 Gif sur Yvette*
*** *FCLAB / FEMTO-ST, Energy Department Rue Thierry Mieg 90010 Belfort Cedex*

Abstract: The energy management issue of a hydrogen fuel cell (FC) with ultracapacitors (UCs) for applications with high instantaneous dynamic power is considered. Singular perturbation approach is employed for the control of two converters and converter losses. The resistance load is considered unknown variable and the proposed controller uses load current and voltage measurements. The convergence of the voltage controller under converter losses is analysed by using Lyapunov theory. According to a significant FC-UCs benchmark, experimental results highlight the interest of the proposed approach and also show the difficulty due to converter losses.

Keywords: Fuel cell, ultracapacitors, power management, energy-shaping, singular perturbation approach, converter losses.

1. PROBLEM STATEMENT

In this paper, we consider the power management issue of hydrogen Fuel Cell (FC) system associated to a reversible impulse energy source (the ultracapacitors) due to the development increasing of electric and hybrid vehicles since 2009. The FC must deliver a slowly varying current, not more than 4A/s for a 0.5kW/12.5V FC Thounthong et al. (2009), and 10A/s for a 20kW/48V FC Corbo et al. (2009) as examples. That is why the FC needs to be associated with auxiliary sources. Nowadays, these auxiliary sources can either be batteries or supercapacitors (UCs). Sometimes, batteries are not able to bear high power charge and discharge conditions, whereas UCS have a high power range. Therefore, for fast power demands, supercapacitors are probably the best-suited components Rodatz et al. (2005). This supply set leads to a design challenge requiring to conceive an adapted architecture, to choose power components, and to dene the appropriate associated control strategy Thounthong et al. (2005).
The parallel structures with only one converter Davat et al. (2009) or two converters Thounthong et al. (2005) can fully respect the mentioned requirements. This paper is dedicated to the study of the structure with two converters as shown in Fig. 1. This architecture offers lower stress for components and an easy and a more reliable power management Cacciato et al. (2004). However it inserts extra weight and complexity (consequently a control challenge). The three major objectives of this power architecture management are to match globally the power (positive or negative) demanded by the load while satisfying FC dynamics (mainly limited by the time response of the air compressor) and monitoring the storage device (UCs) state of charge. It means that the current delivered by the FC must have smooth behaviour in order to ensure its live time, while the UCs provide the load power transient. The hybridization of the electrical supply is highly recommended to limit the dynamic effects and a special attention is also paid for the shut-down and start-up procedures to preserve the fuel cell performances and enhance its durability. Therefore, it seems clear that the DC bus regulation is managed by the ultracapacitors.

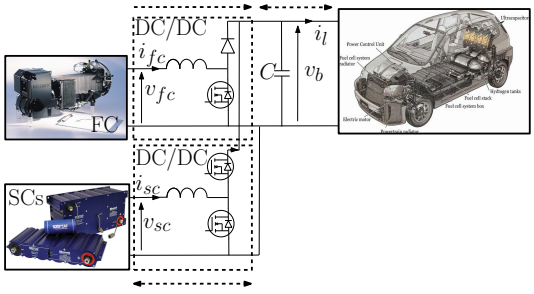


Fig. 1. Two converters parallel structure studied in this work.

To reach the objectives, high-performance controllers are readily available based on the system state Jiang and Dougal (2006), fuzzy logic Kisacikoglu et al. (2009), proportional-integral controllers Thounthong et al. (2009), Davat et al. (2009), RST controller Caux et al. (2005), passivity Becherif (2006), flatness Payman et al. (2008) or model predictive control Vahidi et al. (2006).
Alternative approaches exist such as optimal control Rodatz et al. (2005), dynamic programming Brahma et al.

(2010) or empirical control associated with a multi objective genetic algorithm optimization Paladini et al. (2007) that has been applied for the supervisory power train control problem in charge sustaining hybrid electric vehicles. However, these approaches are based on the *a priori* knowledge of the load, thus real-time control is not straightforward implementable.
The frequency decoupling method using two cascaded loops of currents and voltages proposed in Davat et al. (2009) allows to have fast transient load power provided by the UCs supply, while the FC supplies the mean power (This slow FC dynamics increases the system life time). The control is mainly based on the change in the DC bus voltage induced by load power variations. The controller gains are tuned to ensure the closed-loop system stability, although it has not been theoretically proved.
In Talj et al. (2009) work, a passivity based approach is adopted experimented which enables to prove the closed-loop system stability. However this control is sensitive to the load knowledge. To overcome this drawback, the authors have proposed to use either an observer estimating the unknown resistance load or an integral action.
In Ghanes et al. (2011) a controller based on singular perturbation approach (Khalil (1996), Kokotovic et al. (1986)) is proposed to respect the slower FC dynamics, control of the storage device (UCs) state of charge and the power response required by the load with a DC bus regulation. This solution permits to avoid the use of a PI controller loop which is not very robust to load variation Davat et al. (2009) and the use of an observer or an integral action Talj et al. (2009). Moreover this approach is well adapted to the problem of FC-UCs control where the FC and UCs currents must be slow and fast respectively. A stability proof of the system is given. Nevertheless the converter losses are not taken account in Ghanes et al. (2011).
In this paper, the losses of the two converters used with FC-UCs system are considered. The contribution is to analyse the problem of FC-UCs control in presence of converter losses by the proposed singular perturbation approach. Moreover, experimental results are given to highlight the validity limit of the proposed control against converter losses.

The paper is organized as follows : In section 2, the idea of the singular perturbation (SP) approach is recalled. The FC-UCs model is presented in section 3. In section 4, the proposed controller with a stability proof under converter losses is develloped. Section 5 reports the experimental results. Conclusion and on-going work are given by section 6.

2. BRIEF RECALLS ON SINGULAR PERTURBATION

Let us consider the following nonlinear system:

$$\dot{x} = f(x, z, \varepsilon) \tag{1}$$

$$\varepsilon \dot{z} = g(x, z, \varepsilon) \tag{2}$$

with $x \in R^m$, $z \in R^n$, ε a small positive parameter and f, g two analytical vector fields of appropriate dimension. Roughly speaking, x can be see as the slow state and z as the fast variable. Nevertheless, this statement must be clarified and some assumptions and theoretical developments must be added. First of all, it is usual to decompose the system (1)-(2) in decoupled two time scales dynamic. For this purpose, it is important to be able to compute the so-called slow manifold $z = \phi(x, \varepsilon)$, this manifold is the z behaviour when the fast transient time is finished ("outside the boundary-layer"). The slow manifold ϕ must verify the following equation:

$$\varepsilon \dot{\phi}(x, \varepsilon) = g(x, \phi(x, \varepsilon), \varepsilon) \tag{3}$$

where $\phi(x, \varepsilon) = \sum_{i=0}^{\infty} \alpha_i(x) \frac{\varepsilon^i}{i!}$ is computed iteratively Vasil'eva (1963). For example the so-called frozen solution verify:

$$0 = g(x, \alpha_0(x), 0)$$

Condition is requested for the α_0 existence:
Assumption A.1: The Jacobian $\{\frac{\partial g(x,z,0)}{\partial z}\}$ is regular in the considered state space $x \in D_x \in R^M$ and $z \in D_z \in R^n$.
This assumption is directly linked to the implicit function theorem and in nonlinear case more than one solution is possible (this particular case is outside the scoop of this short presentation). Now, it is important to know if the system (1)-(2) converges on a slow manifold this is given by the well known Tikhonov's theorem Tikhonov et al. (1970) but before recall the theorem it is necessary to analyse the fast dynamic on the boundary-layer. For this, a new state variable $\eta = z - \phi$ is introduced and η converges rapidly to zero if the system behavior converges on the slow manifold. The η dynamics is equal to

$$\dot{\eta} = \frac{1}{\varepsilon} g(x, \phi(x, \varepsilon) + \eta, \varepsilon) - \frac{\partial(\phi(x, \varepsilon), \varepsilon)}{\partial t} \tag{4}$$

Setting $\varsigma = \frac{t}{\varepsilon}$, (4) may be rewritten

$$\frac{\partial \eta}{\partial \varsigma} = g(x, \phi(x, \varepsilon) + \eta, \varepsilon) - \varepsilon \frac{\partial \phi(x, \varepsilon), \varepsilon)}{\partial \varsigma} \tag{5}$$

Assumption A.2 The system (5) is locally in η and uniformly in x exponentially stable.
Hereafter, the Tikhonov's Theorem without considerations of time domain and existence and uniqueness of the solution (for example Lipschitz conditions are implicit).

Theorem 1. Under the assumptions A.1 and A.2 and for $\varepsilon \in R^+$ sufficiently small, after a transient t_1 the dynamics (1)-(2) evolves on a slow dynamic on his dynamic is equal to:

$$\dot{x} = g(x, \phi(x), \varepsilon) \tag{6}$$

In many applications, (6) is approximated at first order (the frozen solution of ϕ)

$$\dot{x} = g(x, \alpha_0(x), 0) \tag{7}$$

As in the considered application the dynamics are too dynamically closed, some fast actuators (high-gain feedback) are used Marino (1985).
Considering, for the seek of simplicity, the following dynamical system

$$\dot{\chi} = \tilde{f}(\chi, \zeta) \tag{8}$$

$$\dot{\zeta} = \tilde{g}(\chi, \zeta) + \tilde{\beta}(\chi) u \tag{9}$$

with $\chi \in R^m$, $\zeta \in R^n$, $u \in R^n$ and $\tilde{\beta}$ regular for all χ. Then setting, for example $u = -\frac{1}{\varepsilon} \tilde{\beta}(\chi)^{-1}(\zeta - \alpha_0(\chi))$ the dynamics become:

$$\dot{\chi} = \tilde{f}(\chi, \zeta) \tag{10}$$
$$\varepsilon\dot{\zeta} = \varepsilon\tilde{g}(\chi, \zeta) - (\zeta - \alpha_0(\chi)) \tag{11}$$

Dynamics (10)-(11) are similar to the dynamics (1)-(2), thus, it is possible to use the theorem 1 and the slow dynamic of (10)-(11) in first approximation is equal to

$$\dot{\chi} = f(\chi, \alpha_O(\chi)) \tag{12}$$

***Remark** 1.* In this paper, we often restrict our purpose to the first approximation of the slow manifold i.e. $\phi \simeq \alpha_O(x)$. Nevertheless, for example, when the system behaviour is too closed to a fold it is necessary to do a better ϕ's approximation.

3. FUEL CELL-ULTRACAPACITORS MODEL: TWO TIME SCALES MODEL

The "fuel cell-ultracapacitors" (FC-UCs) system (figure 2) is modelled by the following 5^{th} order non-linear state space model :

$$\begin{aligned}
\dot{x}_1 &= \frac{(1-\alpha_1)\,x_4 + (1-\alpha_2)\,x_5 - x_3 - i_d}{C} \\
\dot{x}_2 &= -\frac{x_5}{C_{sc}} \\
\dot{x}_3 &= \frac{-R_l\,x_3 + x_1}{L_l} \\
\dot{x}_4 &= \frac{-(1-\alpha_1)\,x_1 + z}{L_{fc}} \\
\dot{x}_5 &= \frac{-(1-\alpha_2)\,x_1 + x_2}{L_{sc}}
\end{aligned} \tag{13}$$

with state space
$x(t) = [x_1, x_2, x_3, x_4, x_5]^t = [v_b, v_{sc}, i_l, i_{fc}, i_{sc}]^t$,
control inputs $u(t) = [u_1;\, u_2]^t = [1-\alpha_1;\, 1-\alpha_2]^t$
and measures $y(t) = x$, $z(t) = v_{fc}$.
Moreover the actual power converter has power losses which has to be taken into account using the term i_d. Current i_d refers to the to the losses current of FC converter (i_{d1}) and UC converter (i_{d2}). These current depend of the main currents (x_4 and x_5) and are expressed as the sum of a linear term and a quadratic term

$$\begin{aligned}
i_d = i_{d1} + i_{d2} = \frac{(V_0 + R_0 x_4)x_4}{x_2} \\
+ \frac{(V_0 + R_0 x_5)x_5}{z}
\end{aligned} \tag{14}$$

where V_0, R_0 represent respectively the threshold voltage and the internal resistance of switches.

4. CONTROL DESIGN

Two fast actuators are applied to the FC-UCs model (13). These fast actuators are implemented with two PI controllers. The dynamics of both PI are chosen such that assumptions A.1-A.2 are verified and hence outside the boundary-layer the dynamic is on the slow manifold and the system behaviour is given by equation (7).

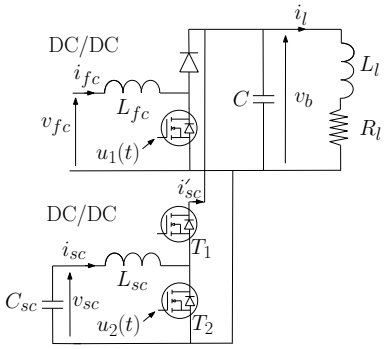


Fig. 2. FC-UCs system.

According to (7), the fast actuators allows to get a slow reduced dynamics of (13) in input-state representation where i^*_{fc} is considered as the input u_1 and i^*_{sc} as the input u_2 :

$$\begin{aligned}
\dot{x}_1 &= \frac{1}{C}\left(\frac{z_3}{x_1}\,u_1 + \frac{x_2}{x_1}\,u_2 - x_3 - i_d\right) \\
\dot{x}_2 &= -\frac{u_2}{C_{sc}} \\
\dot{x}_3 &= \frac{-R_l\,x_3 + x_1}{L_l}
\end{aligned} \tag{15}$$

with $x = [x_1;\, x_2;\, x_3]^t = [v_b;\, v_{sc};\, i_l]^t$; control inputs $u = [u_1;\, u_2]^t = [i^*_{fc};\, i^*_{sc}]^t$, measures $y = [v_b;\, v_{sc};\, i_l]^t$ and $z = [i_{fc};\, i_{sc}, v_{fc}]^t$. The current losses i_d given by (14) is rewritten as follows

$$i_d = \frac{(V_0 + R_0 * u_1)u_1 + (V_0 + R_0 u_2)u_2}{x_1}. \tag{16}$$

It is important to note that the model (15) is valid only if all its outer closed loops dynamics are slower than the dynamics of the fast actuators, namely the PI controllers which assign the current i_{fc} and i_{sc}. This will be a constrain in the design of the slow controllers.

4.1 Slow control design

The desired equilibrium point are the following one $x^* = [v^*_b;\, v^*_{sc};\, \frac{v^*_b}{R_l}]$, with v^*_b and v^*_{sc} the DC bus and UCs desired voltages. As the constraint on i_{fc} is such that its dynamic must be very slow (i.e. $\frac{di_{fc}}{dt} < 10As^{-1}$), u_1 is considered as a slow input and has only a slow effect on the convergence of the dynamic (15). Consequently the gain on the u_1 loop must be very small and the variation of the component of u_1 must be filtered directly or implicitly. From these considerations u_1 is designed as

$$u_1 = \frac{x_1}{z_3} i_{lm} - \frac{C_{cs}}{T_{slow}} e_{sc} \tag{17}$$

where i_{lm} is the load current average (in reality a load's current filtered with a low past filter). Moreover, $e_{sc} = v_{sc} - v^*_{sc}$ and T_{slow} are chosen in order that the feedback on e_{sc} will be also sufficiently slow. It is important to note that e_{sc} is not filtered because v^*_{sc} has a constant profil and v_{sc} is proportional to the i_{sc} integral and then implicitly filtered.

4.2 Fast control design

As u_1 is a slow input the second input u_2 can be faster than u_1 but slower that the current loops driven by both PI fast actuators, so u_2 is:

$$u_2 = \frac{x_1}{x_2}[-\frac{C}{T_{fast}}e_b - \frac{z_3}{x_1}(\frac{x_1}{z_3}i_{lm} - \frac{C_{cs}}{T_{slow}}e_{sc}) + x_3 + i_d] \quad (18)$$

with $e_b = v_b - v_b^*$ and T_{fast} is chosen in order that the feedback on e_b remains slower that both PI fast actuators but faster than the loop on e_{sc}. From (17) and (18), it is possible to set the following proposition.

***Proposition** 1.* Under the controls (17) and (18), the system (15) including converters losses (i_d) is locally exponentially stable for v_b^* and v_{sc}^* constants with a bias on $x_2 = v_{sc}$.

Proof.

Considering the following Lyapunov candidate function $V = V_1 + V_2 + V_3$ with $V_1 = 0.5e_i$, $V_2 = 0.5e_b^2$ and $V_3 = 0.5e_{sc}^2$, where $e_i = (x_3 - i_{lm})^2$ and $i_{lm} = v_b^*/R_l$.

By applying the controls (17)-(18) to the reduced model (15), the differentiation of V gives:

$$\dot{V} = e_i\frac{-R_l e_i + e_b}{L_l} - \frac{e_b^2}{T_{fast}} - e_{sc}\left(\frac{\frac{x_1}{x_2}[\frac{C}{T_{fast}}e_b - \frac{z_3}{x_1}(\frac{x_1}{z_3}i_{lm} - \frac{C_{cs}}{T_{slow}}e_{sc}) + x_3 - i_d]}{C_{cs}}\right)$$

Choosing $T_{fast} << 1$, it follows that e_b converges to zero independently of e_i. Consequently e_i also converges exponentially to zero and this uniformly with respect to e_{sc}. Then

$$\dot{V} = -\frac{R_l}{L_l}e_i^2 - \frac{1}{T_{fast}}e_b^2 - \frac{z_3}{T_{slow}x_2}e_{sc}^2 + \frac{x_1 i_d}{x_2 C_{cs}}e_{sc}$$

Which is locally exponentially stable for $x_2 > 0$ with a bias convergence of e_{sc} to $\frac{x_1 i_d}{x_2 C_{cs}}$ depending on i_d. Moreover T_{slow} must be chosen in order that the dynamic of e_{sc} is slower with respect to PI fast actuators. ■

***Remark** 2.* It is important to note that the bias may be cancelled by adding an adaptive skim. This will be done in a future work. Moreover due to practical implementation, the control is digital and some problems appear due to sampling frequency and quantification Monaco et al. (2011).

5. EXPERIMENTAL RESULTS

To test and validate the performances of the proposed FC controller (17-18), a dedicated FC Control Benchmark is given by Fig. 5-(a)-(c) where the reference DC bus voltage v_b is set equal to 50V and the load current i_l varies between 1 and 20 A. Due to the safety constraints of academic laboratory use, this power cycle is representative of a reduced vehicle power demand, where the load requirement consists in raising and lowering power edges between 50 and 500W.

Experimental set-up.

Fig. 3 shows the experimental set-up used under which the proposed control is tested. The test bench is based on a Nexa fuel cell, Maxwell ultracapacitor bank, a programmable electronic load of 1800 W ($i_{max} = 150A/V_{max} = 60V$) and a dSPACE DS1103 controller board.
The supply sources are interconnected to the DC bus using two choppers built with standard IGBT modules The switching frequency of the PWM is set to 15 kHz. Electric characteristics of both sources are shown in table I.

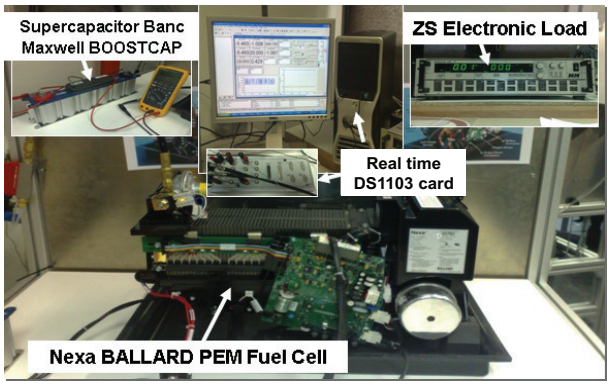


Fig. 3. Experimental set-up.

Block diagram scheme.

The block diagram scheme of the proposed controller is depicted in Fig. 4. It is composed of four subsystems : one fast actuator for the FC based on a PI controller, second actuator to manage the current of the UCs based on a PI controller, the proposed singular perturbation approach to control the DC bus voltage and state of charge of the UCs, and finally the offline identified converter losses.

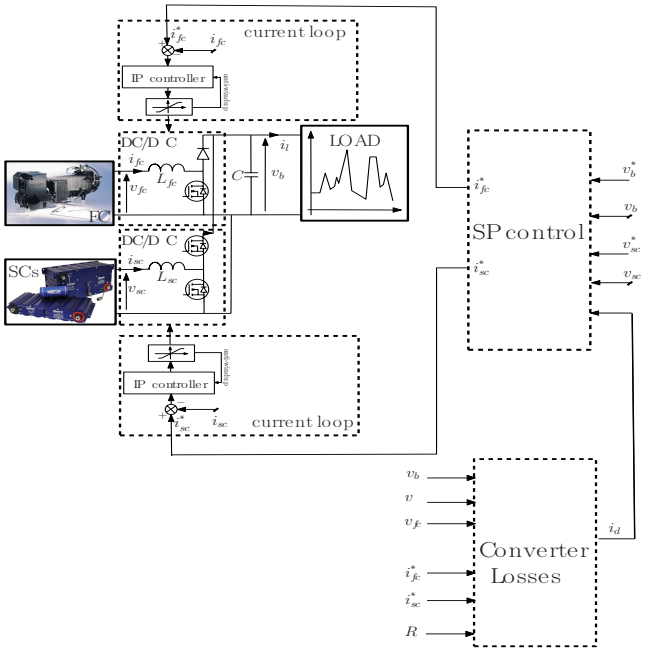


Fig. 4. Singular Perturbation structure with converters losses.

Concerning the load, the proposed FC controller uses only the measurement of load current and load voltage while the resistance load is an unknown variable.

5.1 Experiments without converter losses

Fig. 5 shows the response of the FC hybrid system according to the reference trajectories of a significant Benchmark Fig. 5-a)-b)-f), when the converter losses (16) are not included in controller u_2 (18), i.e. $i_d = 0$. The parameters of u_2 (18) are chosen as follows: $T_{fast} = 50ms$ and $T_{slow} = 2s$. It can be remarked that the DC bus showed by Fig. 5-b) is not well regulated by the proposed fast controller (18) (because of converter losses which are not taking into account) and its value is fluctuate with respect to load current reference. To overcome this difficulty we have tried to decrease the value of T_{fast} but the error of DC bus regulation was near 20% which is not acceptable. Nevertheless a smooth response of the FC current [1] (Fig. 5-(c)) is ensured during fast power demands of the load (Fig. 5-a)) so as to maintain the FC state of health. However, the energy balance is well achieved, characterized by a SC voltage (Fig. 5-f)) value reaching the desired set point (21V) at steady state by the proposed slow controller (17) with a small static error as stated in proposition 1 and demonstrated by proof 4.2.

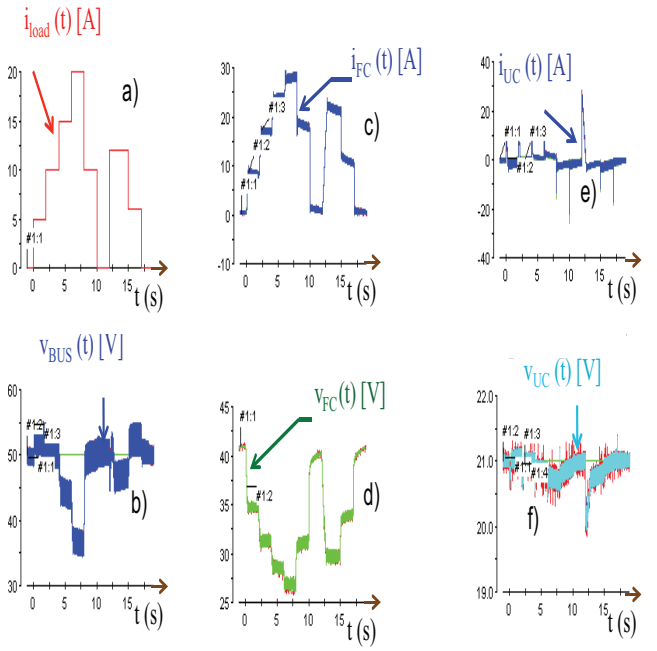


Fig. 5. Experimental results without converter losses. Main variables $(i_L(t), i_{FC}(t), i_{UC}(t), v_{BUS}(t), v_{UC}(t))$ using the two tuning parameters ($T_{fast} = 50ms$ and $T_{slow} = 2s$) and the two bounds ($I_{FCMAX} = 40A$ and $(\frac{di_{FC}}{dt}MAX = 30A/s)$.

5.2 Experiments with offline converter losses identification

In this section, the converter losses i_d are included in the fast controller controller u_2 (18) as showed by Fig. 6. The converter losses are offline identified in steady state conditions. As the load current reference changes from zero to $20A$, then the current converter losses is deduced from equation (16) where $u_{1max} = 45A$, $V_0 = 1,5V$ and $R_0 = 170m\Omega$.

The experimental results of the FC hybrid system according to the significant Benchmark Fig. 6-a)-b)-f) are displayed in Fig. 6. Compared to previous case (without converter losses) it can be noted that the DC bus showed in Fig. 5-b) is now well regulated by the proposed fast controller (18) and its error is less than 2% which is acceptable. The same conclusion is made for FC current and SC voltage (Fig. 6-f)) responses, as done for the case without converter losses.

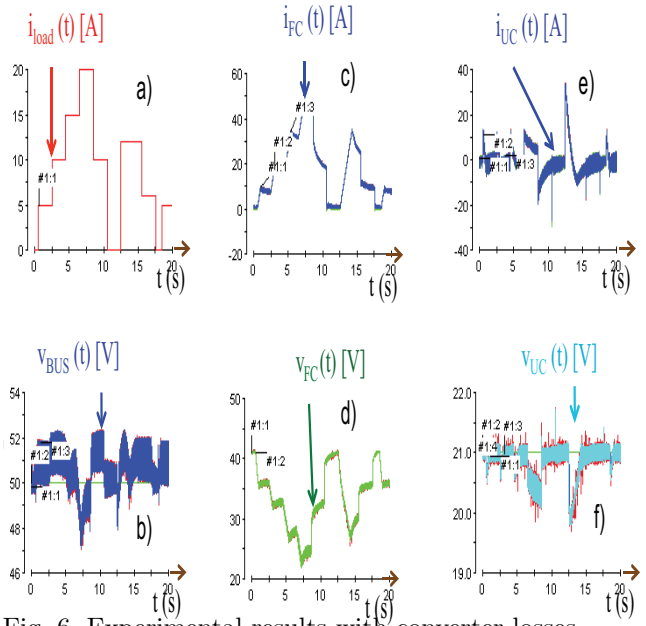


Fig. 6. Experimental results with converter losses. Main variables $(i_L(t), i_{FC}(t), i_{UC}(t), v_{BUS}(t), v_{UC}(t))$ using the four tuning parameters ($V_0 = 3V$, $R = 0,170\Omega$, $T_{fast} = 10ms$ and $T_{slow} = 0,2s$) and the two bounds ($I_{FCMAX} = 40A$ and $(\frac{di_{FC}}{dt}MAX = 30A/s)$.

6. CONCLUSION

Using both singular perturbation control and Lyapunov theory, this article demonstrates that it is possible to prove the stability of the FC/UCs system satisfying unknown variable load. Converter losses are taken into account in this proof. FC and UCs currents have to be slow and fast respectively which is not a major constraint since it respects the devices specifications. The experimental results, presented on a reduced scale test bench representative of a electrical vehicle application, highlight the interest of the proposed approach. However, the obtained results are linked to an off-line method identification test which enables to determine the converter losses. Consequently, our on-going work is to estimate the converter losses on-line using a suitable observer.

Acknowledgment This research was supported by the PEPS project "GESE : Gestion Echantillonne des Systmes Energtiques", 2012.

[1] The FC rate of change is nearly equal to 10A/s as for an FC example given by Thounthong et al. (2009), Corbo et al. (2009)

REFERENCES

Becherif, M. (2006). Passivity-based control of hybrid sources : fuel cell and battery. *IFAC Symposium on Control in Transportation Systems*.

Brahma, A., Guezennec, Y., and Rizzoni, G. (2010). Optimal energy management in series hybrid electric vehicles. *American Control Conference*.

Cacciato, M., Caricchi, F., and Santini, E. (2004). A critical evaluation and design of bi-directional dc/dc converters for supercapacitors interfacing in fuel cell applications. *IEEE Industry Applications Conference*.

Caux, S., Lachaize, J., Fadel, M., Shott, P., and Nicod, L. (2005). Modelling and control of a fuel cell system and storage elements in transport applications. *Journal of Process Control*, 15, 481–491.

Corbo, P., Migliardinia, F., and Veneri, O. (2009). Pefc stacks as power sources for hybrid propulsion systems. *International Journal of Hydrogen Energy*, 34(10), 4635–4644.

Davat, B., Astier, S., Azib, T., and Bethoux, O. (2009). Fuel cell-based hybrid systems. *8th International Symposium on Advanced Electromechanical Motion Systems*.

Ghanes, M., Hilairet, M., Barbot, J., and Bethoux, O. (2011). Singular perturbation control for coordination of converters in a fuel cell system. *Electrimacs*.

Jiang, J. and Dougal, R. (2006). A compact digitally controlled fuel cell/battery hybrid power source. *IEEE Transactions on Industrial Electronics*, 53(4).

Khalil, H.K. (1996). *Nonlinear systems, 2nd edition*. Printice-Hall.

Kisacikoglu, M., Uzunoglu, M., and Alam, M. (2009). Load sharing using fuzzy logic control in a fuel cell/ultracapacitor hybrid vehicule. *International Journal of Hydrogen Energy*, 34, 1497–1507.

Kokotovic, P.V., Khalil, H., and O'Reilly, J. (1986). *Singular Perturbation Methods in control: Analysis and design*. Academic Press, New York.

Marino, R. (1985). High-gain feedback in non-linear control systems. *International Journal of Control*, 42.

Monaco, R., Normand-Cyrot, D., and Tiefensee, F. (2011). Sampled-data energetic management of a fuel cell/capacitor system. *IEEE Transactions on Automatic Control*, 56(4), 907–912.

Paladini, V., Donateo, T., de Risi, A., and Laforgia, D. (2007). Super-capacitors fuel-cell hybrid electric vehicle optimization and control strategy development. *Energy Conversion and Management*, 48(11), 3001–3008.

Payman, A., Pierfederici, S., and Meibody-Tabar, F. (2008). Energy control of supercapacitor/fuel cell hybrid power source. energy conversion and management. *Energy Conversion and Management*, 49(6), 1637–1644.

Rodatz, P., Paganelli, G., Sciarretta, A., de Risi, L., and Guzzella, D. (2005). Optimal power management of an experimental fuel cell/supercapacitor-powered hybrid vehicle. *Control Engineering Practice*, 13(1), 41–53.

Talj, R., Ortega, R., and Hilairet, M. (2009). A controller tuning methodology for the air supply system of a pem fuel-cell system with guaranteed stability properties. *International Journal of Control*, 82(9), 1706–1719.

Thounthong, P., Ral, S., and Davat, B. (2005). Supercapacitors as an energy storage for fuel cell automotive hybrid electrical system. *International Journal of Electrical Engineering in Transportation*, 1(1).

Thounthong, P., Ral, S., and Davat, B. (2009). Energy management of fuel cell/battery/supercapacitor hybrid power source for vehicle applications. *Journal of Power Sources*, 193(1), 376–385.

Tikhonov, A.N., Vasil'eva, A., and Volosov, V. (1970). *Ordinary differential equations*. Springer-Verlag, New York.

Vahidi, A., Stefanopoulou, A., and Peng, H. (2006). Current management in a hybrid fuel cell power system : a model-predictive control approach. *IEEE Transactions on Control Systems Technology*, 14(6).

Vasil'eva, A. (1963). Asymptotic behavior of solutions to certain problems involving nonlinear differential equations containing a small parameter multipling the highest derivatives. *Rusian Math*, 18, 13–18.

Fuel Cell: Parameter Name	Value
Open circuit voltage	$45V$
Rated voltage	$26V$
Rated current	$46A$
Ultracapacitors: Parameter Name	**Value**
Capacitance	$26F$
Rated voltage	$30V$
Rated current	$50A$
Optimal Voltage (V_{UCref})	$50V$
Inductors and Capacities: Parameter Name	**Value**
Inductor L_{fc}	$200\mu H$
Inductor L_{sc}	$100\mu H$
Rated current I_{fc}	$50A$
Rated current I_{sc}	$50A$
Capacities C_{bus}	$14mF$
Optimal DC Bus Voltage (V_{BUSref})	50V

Table I. Electric Characteristics of Hybrid System.